

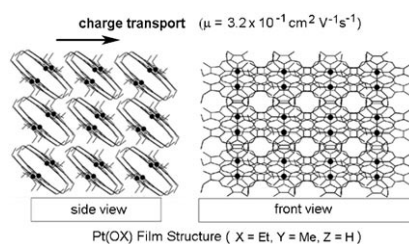
Molecular Electronics

C.-M. Che,* H.-F. Xiang, S. S.-Y. Chui,
Z.-X. Xu, V. A. L. Roy, J. J. Yan, W.-F. Fu,
P. T. Lai, I. D. Williams

A High-Performance Organic Field-Effect Transistor Based on Platinum(II) Porphyrin: Peripheral Substituents on Porphyrin Ligand Significantly Affect Film Structure and Charge Mobility

Chem. Asian J.

DOI: 10.1002/asia.200800011



Shaped up: Organic field-effect transistors incorporating planar π -conjugated metal-free macrocycles and their metal derivatives can be fabricated by vacuum deposition. Annealing the Pt(OX)-based transistor leads to the formation of a well-ordered polycrystalline film that exhibits excellent overall charge transport properties, and has the best value of the charge mobility, μ , reported for a metalloporphyrin.

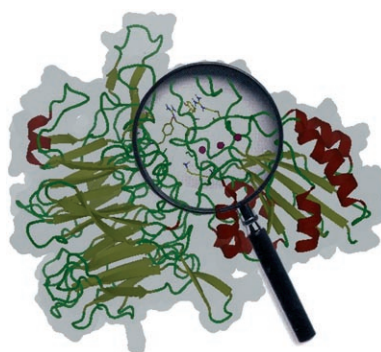
Integrin Ligands

D. Heckmann, A. Meyer, B. Laufer,
G. Zahn, R. Stragies, H. Kessler*

Rational Design of Highly Active and Selective Ligands for the $\alpha 5 \beta 1$ Integrin Receptor

ChemBioChem

DOI: 10.1002/cbic.200800045



Designer ligands: Based on a homology model of the integrin receptor, ligands have been designed and optimised for high affinity for the $\alpha 5 \beta 1$ subtype, and high selectivity against the $\alpha v \beta 3$ subtype. The identification of hotspot mutations allowed the synthesis of new $\alpha 5 \beta 1$ ligands as well as induction of selectivity for formerly nonspecific ligands. The best compounds of the series displayed an IC_{50} value in the low nanomolar range and selectivities that exceeded 8000-fold.

Phthalocyanine Nanotubes

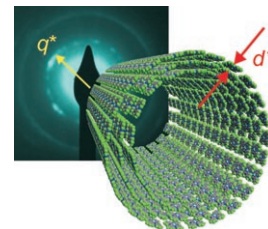
E. Barrena, X. N. Zhang,
B. N. Mbenkum, T. Lohmueller,
T. N. Krauss, M. Kelsch, P. A. van Aken,
J. P. Spatz, H. Dosch*

Self-Assembly of Phthalocyanine Nanotubes by Vapor-Phase Transport

ChemPhysChem

DOI: 10.1002/cphc.200700834

Gold-borne: Phthalocyanine ($F_{16}CuPc$) assembles into multiwalled nanotubes by vapor deposition onto SiO_2 surfaces functionalized by Au nanodots. Their length can be tuned over a large range. The picture shows the wall spacing d^* of a $F_{16}CuPc$ nanotube as deduced from the first diffraction fringe of the electron diffractogram.



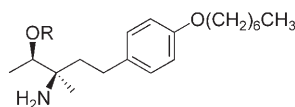
Immunomodulators

K. Högenauer,* A. Billich, C. Pally,
M. Streiff, T. Wagner, K. Welzenbach,
P. Nussbaumer

Phosphorylation by Sphingosine Kinase 2 is Essential for in vivo Potency of FTY720 Analogues

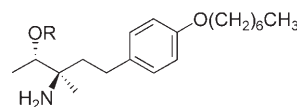
ChemMedChem

DOI: 10.1002/cmdc.200800037



$R = P(O)(OH)_2$: potent S1P1 agonist
 $R = H$: high SPHK2 phosphorylation rate
→ lymphopenia in vivo

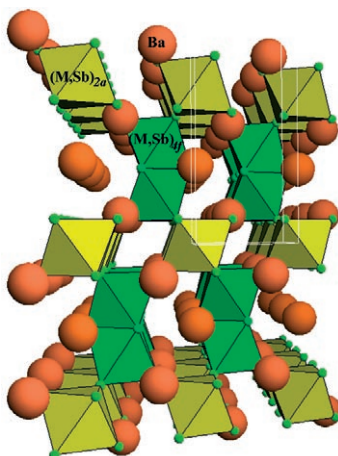
Decisive diastereomers. Sphingosine kinase 2 (SPHK2) phosphorylation rate was found to be the major limiting factor for decreasing peripheral lymphocyte counts of FTY720-like derivatives in vivo.



$R = P(O)(OH)_2$: potent S1P1 agonist
 $R = H$: low SPHK2 phosphorylation rate
→ no lymphopenia in vivo

For a diastereomeric pair of potent S1P1 agonists, lymphopenia was only observed for the epimer showing an efficient SPHK2 phosphorylation rate of the parent amino alcohol.

The crystal structure of the title perovskites can be defined as a 6-layered (6H) hexagonal perovskite structure (space group $P6_3/mmc$) containing dimer units of $(M,Sb)O_6$ octahedra sharing a face along the c axis. The Fe compound shows a severe antisite disordering, whereas the Co perovskite, containing Co^{2+} , is O-deficient, which reduces the disordering. No long-range magnetic ordering was found.



Hexagonal Double Perovskites

M. Retuerto, J. A. Alonso,*
M. J. Martínez-Lope,
M. García-Hernández, K. Krezhov,
I. Spirov, T. Ruskov,
M. T. Fernández-Díaz

Crystal Structure and Magnetism of the 6H Hexagonal Double Perovskites Ba_2FeSbO_6 and $Ba_2CoSbO_{6-\delta}$: A Neutron Diffraction and Mössbauer Spectroscopy Study

Eur. J. Inorg. Chem.
DOI: 10.1002/ejic.200800055



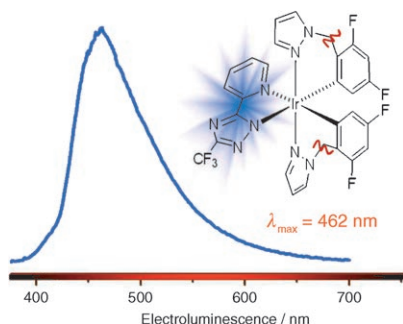
Which one of the two glycosyl donors shown in this picture is more reactive? Conflicting opinions are known. Our approach, which relies on supramolecular aggregation in solutions, can provide a clue to the reasons for the inconsistencies in the literature data on the relative reactivity of sialyl donors.

Glycosylation

L. O. Kononov,* N. N. Malysheva,
E. G. Kononova, A. V. Orlova

Intermolecular Hydrogen-Bonding Pattern of a Glycosyl Donor: The Key to Understanding the Outcome of Sialylation

Eur. J. Org. Chem.
DOI: 10.1002/ejoc.200800324



True blue: The nonconjugated nature of a methylene spacer interrupts the π conjugation of the cyclometalated ligands, which lowers the π orbital energies and destabilizes the respective π^* orbitals. Incorporation of a third chelating chromophore with a blue-light energy gap induces true-blue-light emission at room temperature (see figure).

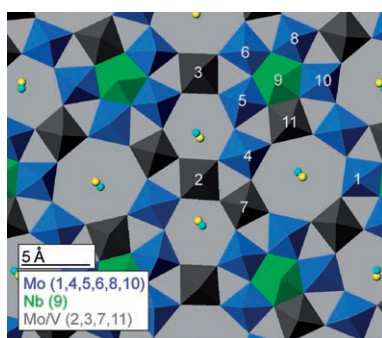
Light-Emitting Diodes

Y.-H. Song, Y.-C. Chiu, Y. Chi,*
Y.-M. Cheng, C.-H. Lai, P.-T. Chou,*
K.-T. Wong, M.-H. Tsai, C.-C. Wu*

Phosphorescent Iridium(III) Complexes with Nonconjugated Cyclometalated Ligands

Chem. Eur. J.
DOI: 10.1002/chem.200800050

A friendly phase: Bulk mixed-metal Mo-V-Te-Nb oxides are highly promising catalysts for the environmentally friendly selective ammoxidation of propane to acrylonitrile and oxidation of propane to acrylic acid. In this context, the crystal structures and catalytic behavior of Mo-V-Te-Nb-O, Mo-V-Te-O, and Mo-V-O M1 phase catalysts have been studied.



Heterogeneous Catalysis

N. R. Shiju, V. V. Guliants,
S. H. Overbury, A. J. Rondinone*

Toward Environmentally Benign Oxidations: Bulk Mixed Mo-V-(Te-Nb)-O M1 Phase Catalysts for the Selective Ammoxidation of Propane

ChemSusChem
DOI: 10.1002/cssc.200800039